A New Approach to the Nonlinear Spectroscopic Investigation of Dynamics in Complex Solids: Theory and Experiments

Nonlinear optical dephasing experiments and theoretical analysis are described for complex condensed matter systems, e.g., glasses, complex crystals, or proteins. Unlike simple crystals, such systems undergo dynamical processes which have a very broad relaxation rate distribution. Dynamics can occur on a variety of time scales ranging from subpicoseconds to thousands of seconds. The results of optical dephasing measurements (time domain) or linewidth measurements (frequency domain) depend on a time, T_W, which defines the time scale associated with the particular experimental technique. Detailed information about the system's relaxation rate distribution is obtained from the change in the optical dephasing rate as the experimental time scale is changed, not from the dephasing rate (linewidth) measured in any individual experiment. For glasses and similar systems, a fundamental result, which is independent of the nature of the relaxation rate distribution or the coupling to the optical center, is that the derivative of the optical dephasing rate with respect to T_W is directly proportional to the Laplace transform of the relaxation rate distribution. As examples, two types of solids are considered, optical centers in a glass and in a complex crystal. For the crystalline system, Pr^{+3}:CaF_2, T_W dependent optical dephasing data from the literature is analyzed quantitatively, where previously only a qualitative description was possible.

I. INTRODUCTION

In this paper we will discuss a newly developed general spectroscopic approach to the investigation of materials with complex dynamics. Our discussion will focus principally on glassy systems, although a complex crystal system, Pr^{+3}:CaF_2, will also be discussed as an example. The method can readily be extended to

Comments Cond. Mat. Phys.
1989, Vol. 14, No. 6, pp. 343–364
Reprints available directly from the publisher
Photocopying permitted by license only

other complex systems such as macromolecules. While we will only discuss optical spectroscopy, the method can readily be applied to other types of spectroscopic techniques, such as NMR.

In a simple crystal, dynamics involve fast phonon induced fluctuations about an equilibrium structure. In a glass, in addition to phonon fluctuations about quasi-static local structures, evolution of the local structures occurs over a vast range of time scales. The constantly changing local structures cause a glass's physical properties, such as the heat capacity and thermal conductance, to be markedly different at low temperatures ($\sim$1 K) from those of crystals.[1] Anderson and co-workers and Phillips independently proposed a model based on the two-level system (TLS) to explain these differences.[2,3] TLS represent extra degrees of freedom that are characteristic of the glassy state, and they contribute a term approximately linear in temperature to the temperature dependence of the heat capacity. Briefly, a TLS is composed of two separate local potential minima separated by a barrier. Changes in local glass structure are modeled as transitions between the two potential minima. A wide distribution of energy differences of the TLS potential minima exist, and a wide distribution of tunneling parameters are responsible for the transitions. As a result, there is a very wide range of time scales associated with the dynamics of the TLS.

The dynamics in a glass can be probed by optical experiments on guest molecules embedded in the glassy host matrix. Thermally induced fluctuations in the local environments induce time-dependent perturbations of the energy levels of the ensemble of guests, and therefore change the transition frequencies between levels. When the transition of interest is in the optical frequency range, the guests are referred to as optical centers. Because of the local fluctuations, each optical center experiences a random dynamical modulation of its transition frequency. If an ensemble of optical centers is coherently prepared at time, $t = 0$, i.e., the optical centers are placed in a coherent superposition of their ground state and an excited electronic state, the random modulations of the transition energy will cause the initially well defined phase relationship among superposition states to decay for $t > 0$. This is referred to as *optical dephasing*. The rate of the dephasing process is determined by the nature of the local fluctuations. Thus by studying the dephasing behavior of the optical centers, one can

gain valuable information about the dynamics of the glass system. In time domain experiments, optical dephasing is studied directly. In frequency domain experiments, which are related to the time domain by Fourier transform relationships, optical dephasing determines experimental line shapes. Optical dephasing experiments also reveal details of the coupling of the medium to the electronic states of the optical centers[4] and can provide information about the structure and the dynamics of solvent shells surrounding the optical centers in the glassy solution.[4]

In the last few years, optical dephasing in low temperature glasses has been studied extensively.[4] Like the heat capacity and other thermal properties, the optical dephasing behavior of glasses is also found to be markedly different at low temperatures ($\sim$1 K) from those of crystals. The dephasing rate increases approximately linearly with temperature and closely resembles the temperature dependence of the heat capacity. This suggests that the dephasing is induced by the same dynamics that govern the low temperature behavior of the heat capacity, i.e., the dynamics of the TLS.

The variety of spectroscopic techniques makes optical dephasing measurements more versatile, hence potentially more powerful, than heat capacity measurements in the study of glass dynamics. The key, however, is to properly link the optical techniques to the dynamics in glassy and other complex condensed matter systems. As will be seen, the new approach, which is briefly described here, provides the direct connection between the nonlinear spectroscopic observables and the details of the microscopic dynamics in complex condensed matter systems.[5]

II. OPTICAL DEPHASING IN CONDENSED MATTER SYSTEMS

The simplest dephasing measurement is the linear absorption measurement. It can be related to system dynamics through Kubo's lineshape theory,[6] i.e., the absorption spectrum is proportional to the Fourier transform of the dipole correlation function (which is a two time or two "point" correlation function),

$$I(\omega_L - \omega_0) \propto \int dt \exp[i(\omega_L - \omega_0)t] \langle \mu(t)\mu^*(0)\rangle, \qquad (2.1)$$

where $\omega_L - \omega_0$ is the detuning of the laser frequency from the transition frequency of the optical centers, and the μ is the transition dipole moment. The dynamics of the environment are modeled as time-dependent stochastic processes that perturb the motion of the dipole. The dipole correlation function is given by

$$\langle \mu(t)\mu^*(0) \rangle = \langle \exp[-i\int_0^t \Delta(t')dt'] \rangle,$$

where $\Delta(t')$ is the time-dependent perturbation of the transition frequency. Information about dynamics of the environment can thus be extracted through the dipole correlation function.

In a condensed matter system at low temperatures, however, transition frequencies of the optical centers are detuned by random static perturbations such as strains or electrical fields. Thus, the transition frequencies are *inhomogeneously broadened*. This means the actual absorption spectrum is the average of Eq. (2.1) over a broad distribution of the transition frequencies. In a glass, the inhomogeneous broadening is typically 4 to 5 orders of magnitude larger than the excited state lifetime limited linewidth. The absorption lineshape of optical centers in a glass is totally dominated by the inhomogeneous broadening and does not give information about the dynamics of the system. This is also true for other condensed phase systems, such as crystals and proteins.

A variety of *nonlinear* spectroscopic techniques have been developed to remove the inhomogeneous broadening. These include two pulse photon echoes,[7] stimulated echoes,[8] accumulated grating echoes,[9,4] incoherent echoes,[10] fluorescence line narrowing,[11,4] saturation optical hole burning,[12] and persistent optical hole burning.[13,4] A common feature of these techniques is that they all measure a linewidth which is narrower than the inhomogeneously broadened absorption line. Thus, they are often referred to as line narrowing experiments. Traditionally, the relation between the lineshapes measured by these line narrowing techniques and the system dynamics is considered to be the same as that given in Kubo's theory.[14] All of these techniques would thus be expected to measure the same linewidth, which is commonly referred to as the "homogeneous linewidth," $\Delta\nu_H$. When the lineshape is Lorentzian, its Fourier transform is an exponential function in the

time domain. The decay constant of the exponential is known as the "homogeneous dephasing rate," $1/T_2 = 1/\pi\Delta\nu_H$. In simple crystals, this is indeed the case.[15]

Recent optical dephasing experiments on glasses[16,17] and on complex crystals,[18] however, have proven that the various techniques, when applied to the same sample, do not measure the same optical dephasing rate. For example, it is found that low temperature (<5 K) optical dephasing rates of resorufin molecules in ethanol glass measured by persistent hole burning are significantly different from those measured by two pulse photon echoes.

In Fig. 1, the resorufin dephasing times measured by these two techniques are plotted as a function of temperature. The spectral shape of the holes is Lorentzian, and the decays of the two pulse echoes are exponential. The dephasing time is related to the hole width (FWHM) by $T_2 = 2/\pi\Delta\nu_H$.[4,17] At low temperature, the temperature dependence of both curves is approximately $T^{-1.5}$.[17] As the temperature is increased, a pseudolocal phonon mode begins to contribute to the dephasing, and at sufficiently high temperature, the curves coalesce.[17] As can be seen, at low temperature, the dephasing rate derived from hole width measurement is as much as a factor of 5–6 larger than that measured by two pulse echo. This difference cannot be explained by Kubo's lineshape theory.[6]

III. THE FOUR-POINT CORRELATION FUNCTION DESCRIPTION OF DEPHASING

Detailed theoretical analyses[17,19,20] have proven that commonly used nonlinear line narrowing techniques should be described in terms of four-point correlation functions, rather than the two-point dipole correlation function used in Kubo's absorption lineshape theory. For example, the dephasing of a stimulated echo is described by the four-point correlation function,

$$C(\tau,T_W,\tau) = \langle\mu^*(T_W + 2\tau)\mu(T_W + \tau)\mu(\tau)\mu^*(0)\rangle$$

$$= \langle\exp[-i\int_0^{\tau}\Delta(t')dt' + i\int_{T_W+\tau}^{T_W+2\tau}\Delta(t')dt']\rangle, \qquad (3.1)$$

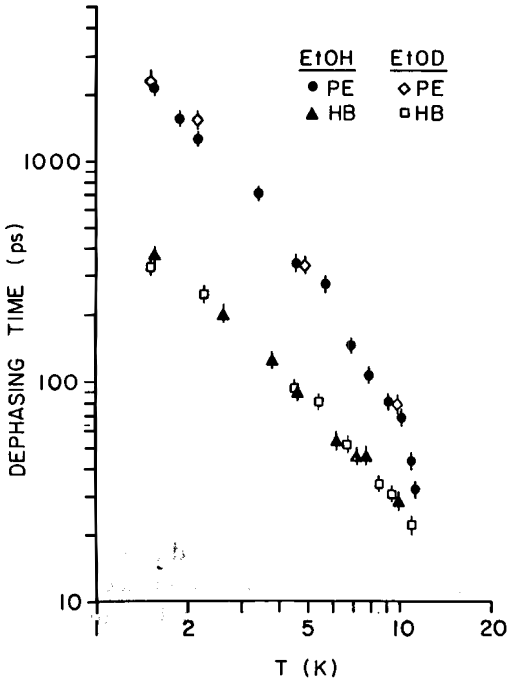

FIGURE 1 Log–log plots of temperature dependent hole burning dephasing times ($2/\pi\Delta\nu_H$) compared to photon echo dephasing times for resorufin in ethanol glasses. The excited state lifetime contributions to both types of measurements have been removed. At low temperatures, the temperature dependence is approximately $T^{-1.5}$ for both measurements. However, the values of the dephasing times at a fixed temperature point differ by a factor of 5–6. At high temperatures, dephasing is dominated by pseudolocal phonons, and the data from the two measurements coalesce. Data taken on regular ethanol (EtOH) glass as well as on a glass of ethanol with the hydroxyl hydrogen replaced with deuterium (EtOD) are found to be identical. This demonstrates that hydrogen bond strength does not play a role in the temperature dependent dephasing (Ref. 17).

where τ is the time delay between the first and the second input laser pulses, and T_W is the time delay between the second and the third input laser pulses.

It has also been proven[17,21] that, in addition to the stimulated echo, all other techniques mentioned in Section II can be described in terms of this four-point correlation function. For example, the

four-point correlation function describing a two pulse echo is the limiting form of Eq. (3.1) with $T_W = 0$. Whereas, for a persistent hole burning measurement, the spectrum of the hole is given by the Fourier transform of Eq. (3.1),

$$I_H(\omega_R - \omega_B) \propto \int d\tau \exp[i(\omega_R - \omega_B)\tau]\, C(\tau, T_W, \tau), \quad (3.2)$$

where ω_R (ω_B) is the reading (burning) laser frequency.

We note that the spectrum of the hole, which is often erroneously considered to be the *homogeneous* lineshape,[4] is generally dependent on a characteristic time scale, T_W, which we will refer to as the "waiting time." For short hole burning and reading times, T_W is the time interval between burning and reading the hole. This is in contrast to Eq. (2.1), which is independent of experimental time scales. As will be seen, it is this T_W-dependence that causes measured lineshapes (or dephasing rates) to vary with different techniques for systems in which the dynamics span a broad range of time scales.

In simple crystals, the dephasing is induced by phonons.[15] Under most experimental conditions, the fluctuation rate associated with the phonon bath is known to be much larger than the measured dephasing rate, which is roughly equal to $1/\tau$. The time-dependent perturbations $\Delta(t')$ within the two time intervals, $[0,\tau]$ and $[T_W + \tau, T_W + 2\tau]$, can be taken as uncorrelated stochastic processes, i.e.,

$$\langle \exp[-i\int_0^{\tau} \Delta(t')dt' + i\int_{T_W+\tau}^{T_W+2\tau} \Delta(t')dt'] \rangle = \langle \exp[-i\int_0^{\tau} \Delta(t')dt'] \rangle^2. \quad (3.3)$$

Thus in a simple crystal, all the line narrowing techniques measure the same lineshape, independent of the waiting time T_W.

In complex systems, the problem is fundamentally different. In addition to phonon induced dephasing, optical dephasing can be induced by the time evolution of local structures. The evolution of local structures in a glass is described in terms of the TLS.[4] The time-dependent perturbations, $\Delta(t')$, are induced by the relaxations of the individual TLS between their two stationary states.

The relaxations can occur on many time scales. When the relaxation rate of the TLS are slower than the optical dephasing rate, the time-dependent perturbations, $\Delta(t')$, within the two time intervals, $[0,\tau]$ and $[T_W + \tau, T_W + 2\tau]$, are correlated. The degree of the correlation is determined by the waiting time, T_W. For a two pulse echo, perturbations with correlation times longer than τ appear to be static inhomogeneous broadening and do not contribute to the optical dephasing. For line narrowing techniques with finite waiting time $T_W >> \tau$, however, the same perturbations can make significant contribution to the measured optical dephasing rates. This argument qualitatively explains the difference between the dephasing rates measured by two pulse photon echoes and persistent hole burning in the resorufin/ethanol glass, where τ is typically picoseconds to nanoseconds and T_W is on the order of tens of seconds.

Thus in complex systems, the term "homogeneous linewidth," which is often taken to be the linewidth measured in any line narrowing experiment, is not well defined. Because the two pulse photon echo is the only optical line narrowing experiment with $T_W = 0$, it will measure the slowest dephasing rate. The dephasing rate measured by the two pulse echo has been used as the operational definition of the homogeneous linewidth.[17,20]

IV. RELAXATION RATE DISTRIBUTION OF THE TLS

A system's complex dynamics, which span a wide range of time scales, can be quantitatively described by a distribution of fluctuation rates. In most cases, the fluctuations are caused by a large number of weakly coupled, localized perturbers, as for example the TLS in a glass. The total perturbation is the sum of independent perturbations induced by each of the individual perturbers,

$$\Delta(t') = \sum_j \Delta_j(t'). \tag{4.1}$$

The fluctuation rate distribution refers to the individual perturbers. In these cases, Eq. (3.1), hence the entire dephasing problem, can be solved exactly.[5] In particular, if the perturbation is induced by

the TLS so that the motion of an individual perturber can be described by "sudden jumps" between two energy levels,[22] one can show that the ratio between the dephasing rate measured by hole burning and that measured by two pulse echoes is[5,21]

$$\Gamma_{HB}/\Gamma_{TPE} = 1 + (1/\Theta)\,\langle 1 - \exp(-RT_W)\rangle_R > 1,$$

where $\Theta \simeq 3.6$.[23] The fluctuation rates correspond to the relaxation rates of the TLS. The average is over the relaxation rate distribution of the TLS with an upper limit, $R_{max} = 1/\tau \sim \Gamma_{TPE}$,

$$\langle 1 - \exp(-RT_W)\rangle_R = \int_0^{1/\tau} dR\, P(R)\,[1 - \exp(-RT_W)]. \quad (4.3)$$

In the standard model,[2,3] the TLS is described by an energy separation E and a tunneling parameter λ, both having flat distributions over broad ranges. At low temperatures, the relaxation of the TLS is predominantly induced by resonant single phonon scattering, $R \propto e^{-2\lambda}$, which, when combined with a flat distribution of λ, directly leads to a relaxation rate distribution of $P(R) \propto 1/R$.[23,24] This result is consistent with the experimentally observed exponential decay of the echo signal,[16,25] which *requires* $P(R) \propto 1/R$ at least in the range of $R \sim \Gamma_{TPE}$.[17,23,26]

Using a relaxation rate distribution of $1/R$ and noting that the square bracket in Eq. (4.3) sets a lower limit on R at $1/T_W$, one can approximately evaluate Eq. (4.2) as[17,21]

$$\Gamma_{HB}/\Gamma_{TPE} = \{\Theta + \ln(\Gamma_{TPE}T_W)\}/\Theta.$$

For the resorufin/ethanol glass system, the photon echo dephasing rate is on the order of a nanosecond, while the waiting time in a hole burning measurement, T_W, is typically 100 seconds. Substituting these numbers into Eq. (4.4), we have $\Gamma_{HB}/\Gamma_{TPE} = 8$, in comparison to the observed value of ~5–6. Thus the simplest model of the relaxation rate distribution in glasses predicts a ratio which is within a factor of 2 of the observed value.

An explanation for the difference between the observed and calculated ratios is that the $1/R$ distribution does not hold for slow relaxation rates.[21] The relaxation rate distribution falls to zero at

a certain cut-off rate, R_{min}, that corresponds to a maximum cut-off, λ_{max}, in the tunneling parameter distribution. Consequently, Eq. (4.4) becomes

$$\Gamma_{HB}/\Gamma_{TPE} = \{\Theta + \ln(\Gamma_{TPE}/R_{min})\}/\Theta. \tag{4.5}$$

For $\Gamma_{HB}/\Gamma_{TPE} = 5$, a model with a sharp cut-off in the relaxation rate distribution gives $R_{min} = 1\ ms^{-1}$. This is an experimentally accessible time scale for fast hole burning experiments and measurements are currently in progress.

It is unlikely that the relaxation rate distribution follows strictly a $1/R$ form and goes to zero at an abrupt cut-off rate. Dynamics occurring in a glass are complex. The nature of the dynamical processes in the system are unknown. The problem is to probe the actual behavior of the relaxation rate distribution, and hence extract information on the dynamics occurring in the medium through the influence of dynamics on the dephasing of the embedded optical centers.

V. PROBING FLUCTUATION RATE DISTRIBUTIONS IN COMPLEX SYSTEMS

In general, the dephasing of optical centers is determined by two factors: the coupling strength between the optical centers and the perturbers, and the fluctuation rate distribution of the perturbers. While the former is an extrinsic property introduced by the doping of the optical centers, the latter usually belongs to the intrinsic dynamics of the host matrix. Previously, an experimental approach that allows the direct measurement of fluctuation rate distributions did not exist. From our discussion in the last section, however, we see that the optical dephasing rate (or the linewidth) is dependent on the characteristic waiting time, T_W, in a measurement. If one can continuously scan the T_W through a broad range and measure the dephasing rate as a function of T_W, it is possible to experimentally map out the fluctuation rate distributions.

In fact, we have shown[5] that waiting time-dependent dephasing measurements can be used to reveal fluctuation rate distributions, and hence dynamics in complex systems. For *two-level type per-*

turbers, whose fluctuations can be described by the sudden jump model,[22] a general relation between an experimental observable and the relaxation rate distribution of the perturbers is found to be[5]

$$\frac{\partial \ln(I_s)}{\partial T_W} \propto \int dR\, P_1(R) \exp(-RT_W),$$

where I_s is the signal intensity of a *stimulated echo*, and $P_1(R) = RP(R)$. This result is independent of the details of the coupling and spatial distribution of the perturbers in the medium to the optical center.

It is worth noting that $P_1(R)$ is the relaxation rate distribution on the $\ln R$-scale, $P_1(R)d(\ln R) = P(R)dR$. In disordered systems, the fluctuation spectra of macroscopic observables are often of the form of $1/f$, over a broad range of frequencies, f. This implies that the relaxation rate distributions are of the form of $1/R$.[27] This universal feature can be attributed to the fact that the relaxation rates in disordered systems are related to microscopic variables σ by $R \propto e^{-\sigma}$. Even a moderately broad distribution of σ will result in a relaxation rate distribution of the form of $1/R$ over several orders of magnitude. The relaxation rate distribution on the $\ln R$-scale is directly proportional to the distributions of the microscopic variables. Thus it is useful to discuss $P_1(R)$ since it is the relaxation rate distribution on the $\ln R$-scale.

Lorentzian lineshapes are commonly observed by optical line narrowing experiments (frequency domain dephasing experiments) in low temperature glasses. Lorentzian lineshapes can result from dipole–dipole coupling to the optical centers and uniform spatial distribution of the TLS (perturbers). For Lorentzians, Eq. (5.1) becomes

$$\frac{\partial(\Delta\nu)}{\partial T_W} \propto \int dR\, P_1(R) \exp(-RT_W),$$

i.e., the derivative of the linewidth with respect to the waiting time T_W is directly proportional to the Laplace transform of the relaxation rate distribution function. Analogous relationships for other models of the fluctuations, e.g., Gaussian fluctuations, have also been obtained.[5]

Other line narrowing techniques, such as transient hole burning[28] and accumulated echoes, can also be used to measure the waiting-time-dependent optical dephasing. Similar relations between these measurements and the relaxation rate distributions have been established.[5] For example, transient hole burning, the frequency domain equivalent of the stimulated echo, is related to the stimulated echo decay function through a Fourier transform.[17] One can relate the result of a waiting-time-dependent hole burning measurement (burn the hole, wait time, T_W, read the hole) to the relaxation rate distribution by replacing I_S in Eq. (5.1) with the inverse Fourier transform of the hole shapes.[5] Relationships between the results of other experiments and the relaxation rate distribution can be established in a similar manner.[5]

We note that the phenomenon described here is quite similar to the spectral diffusion in spin resonance studies.[20,22,29] The key difference is that in spin resonance studies, one deals with fluctuations induced by spin flips at a single rate R_0, whereas we are dealing with a *distribution* of relaxation rates. Further, most spectral diffusion studies are restricted to the short waiting time limit, $R_0 T_W << 1$. As a result, the diffusion rate is commonly found to be a constant,[20]

$$\partial(\Delta\nu)/\partial(T_W) \propto R_0,$$

independent of T_W. One can readily derive this limiting form from Eq. (5.2).

VI. APPLICATIONS TO COMPLEX CONDENSED MATTER SYSTEMS

VI.1. TLS Relaxation Rate Distribution in Glasses

It is commonly assumed that optical dephasing in glasses is caused by TLS. Therefore, the fluctuation rate distribution is the relaxation rate distribution of the TLS. Using the standard TLS model[2,3] one can show that on a log scale, the relaxation rate distribution $P_1(R)$ is essentially a constant in the range from $(\text{ms})^{-1}$ to $(\text{ps})^{-1}$.[21] In Section IV, we estimated that the lower cut-off rate, R_{min}, of the relaxation rate distribution is about 1 $(\text{ms})^{-1}$ for the system resorufin in ethanol glass. It is unlikely, however, that $P_1(R)$ falls

to zero abruptly at R_{min}. It is possible for $P_1(R)$ near R_{min} to behave in a variety of ways. Using waiting-time-dependent dephasing measurements, one can determine the behavior of the relaxation rate distribution in the cut-off region.

Consider the following scenarios for the fall off of the relaxation rate distributions. (1) The relaxation rate distribution suddenly goes to zero at R_{min},

$$P_1(R) = AH(R_{max} - R)\, H(R - R_{min}),$$

where A is a normalization factor, $A = \ln(R_{max}/R_{min})$. R_{max} is the upper limit of the relaxation rate distribution and is assumed to be much larger than the measured dephasing rate.

(2) The relaxation rate distribution falls to zero as a Gaussian function,

$$P_1(R) = A\{H(R_{max} - R)H(R - R_0) + H(R_0 - R)\exp(-[\ln(R/R_0)/\sigma]^2)\},$$

where $R_0 > R_{min}$, and σ is given by

$$\sigma = (2/\sqrt{\pi})\ln(R_0/R_{min}).$$

All the parameters have the same values as those in Eq. (6.1). σ and R_0 are chosen in such a way that the total area covered by this relaxation rate distribution is the same as that covered by the step function distribution in Eq. (6.1). We note that the Gaussian here refers to a Gaussian function on the ln$R$-scale.

(3) The relaxation rate distribution falls to zero exponentially,

$$P_1(R) = A\{H(R_{max} - R)H(R - R_0) + H(R_0 - R)\exp[\ln(R/R_0)/\sigma]\}, \quad (6.3)$$

where $\sigma = \ln(R_0/R_{min})$, and all other parameters have the same values as those in Eq. (6.2). With these parameters, the area covered by this distribution function is the same as that in cases (1) and (2).

All three relaxation rate distribution functions are plotted in Fig. 2(a). The parameters used in the plot are: $R_{max} = 10^{11}\ s^{-1}$,

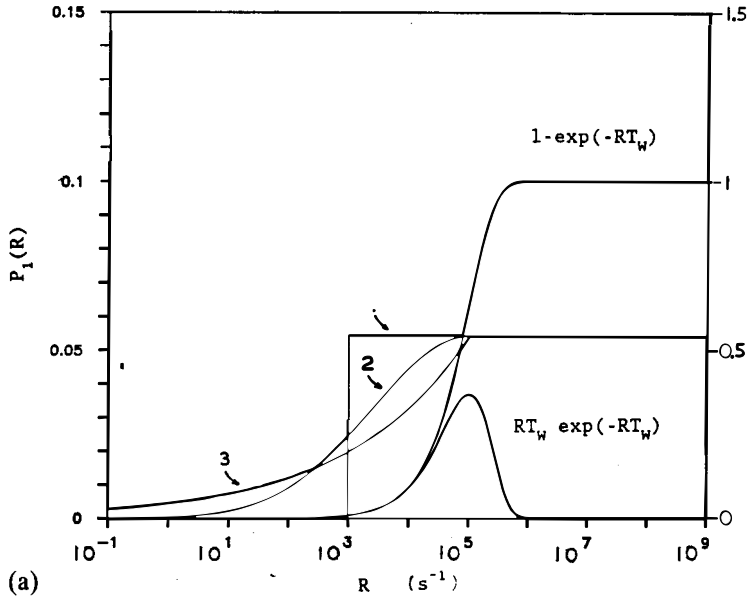
0.15
0.1
0.05
0
1.5
1
0.5
0
$P_1(R)$
$1-\exp(-RT_W)$
$RT_W \exp(-RT_W)$
1
2
3
10^{-1}
10^{1}
10^{3}
10^{5}
10^{7}
10^{9}
R (s^{-1})

(a)

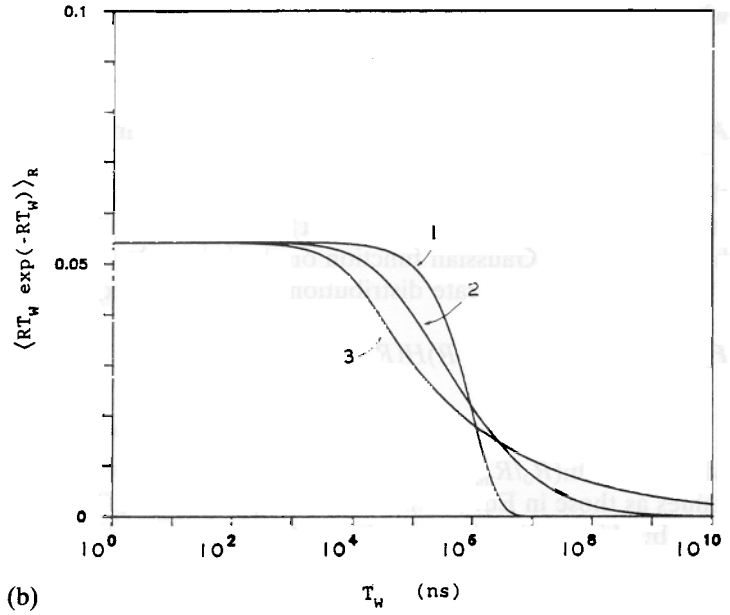
0.1
0.05
0
$\langle RT_W \exp(-RT_W) \rangle_R$
1
2
3
10^{0}
10^{2}
10^{4}
10^{6}
10^{8}
10^{10}
T_W (ns)

(b)

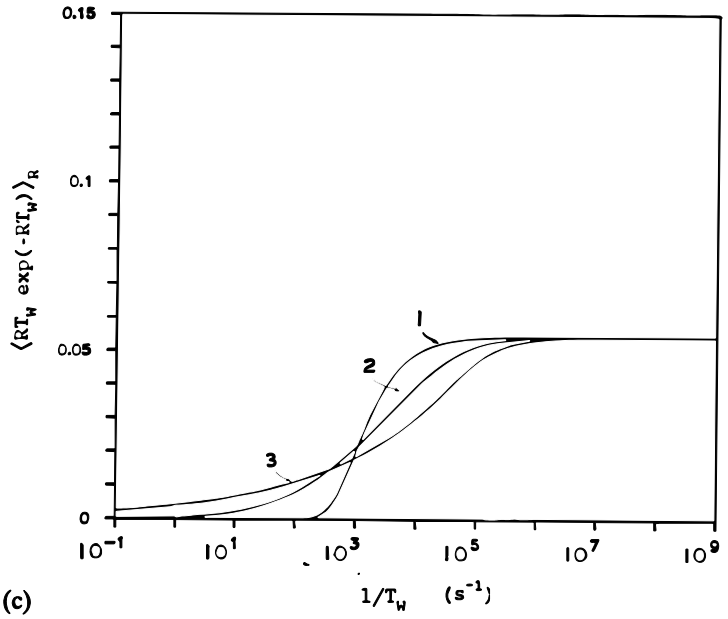

FIGURE 2 (a) Model relaxation rate distributions, $P_1(R)$, for a glass (left scale). The cut-offs at the low fluctuation rates are assumed to be (1) a step function; (2) a Gaussian function; and (3) an exponential function (see text). The parameters used in the plot are: $R_{max} = 10^{11}\,s^{-1}$, $R_{min} = 10^{3}\,s^{-1}$, $R_0 = 10^{5}\,s^{-1}$. As a reference, we also plot the function, $1 - \exp(-RT_W)$, and its derivative, $RT_W \exp(-RT_W)$, at a fixed waiting time $T_W = 10\ \mu s$, showing the effect of scanning T_W (right scale). At a particular T_W, the linewidth measured by a stimulated echo is proportional to the area under the function, $1 - \exp(-RT_W)$. The rate of increase with T_W of the linewidth is proportional to the area under the function $RT_W \exp(-RT_W)$. (b) Plot of $\langle RT_W \exp(-RT_W) \rangle_R$ as a function of T_W. This plot is equivalent to the derivative of the linewidth versus the waiting time T_W. When T_W is short, the derivative of the linewidth is a constant. When T_W is in the region of the cut-off in the relaxation rate distribution, the derivative is changing rapidly. When T_W is long, the derivative goes to zero, i.e., the linewidth is no longer changing with increasing T_W. These plots show that different forms of the relaxation rate distribution function could be readily distinguished. (c) Figure 2b is re-plotted on a $1/T_W$ scale. Note the similarity between this plot and the corresponding relaxation rate distributions in Fig. 2(a). If the relaxation rate distribution falls off relatively slowly, the data is essentially the relaxation rate distribution. Only curve 1, the step function distribution, shows appreciable modification of the underlying relaxation rate distribution function.

$R_{min} = 10^3\ s^{-1}$, $R_0 = 10^5\ s^{-1}$. As a reference, we also plot the function, $1 - \exp(-RT_W)$, and its derivative, $RT_W \exp(-RT_W)$, at a fixed waiting time $T_W = 10\ \mu s$, showing the effect of scanning T_W. The time delay between the first two pulses is assumed to satisfy the condition $T_W/\tau >> 1$. The linewidth measured by a stimulated echo or a transient hole burning experiment is proportional to the area under the function, $1 - \exp(-RT_W)$. At a particular T_W, the rate of increase with T_W of the linewidth is proportional to the area under the function $RT_W \exp(-RT_W)$.

The derivative of the linewidth with respect to $\ln T_W$, according to Eq. (5.2), is proportional to the average of the function $RT_W \times \exp(-RT_W)$. In Fig. 2(b), we plot $\langle RT_W \exp(-RT_W)\rangle_R$ as a function of T_W. This plot is the change of the linewidth versus waiting time, T_W. In all three cases, at short waiting time, $T_W << 1/R_{min}$, the change of the linewidth is a constant. At long waiting time, $T_W >> 1/R_{min}$, the change in the linewidth becomes zero. As T_W is scanned through the region $(1/R_0, 1/R_{min})$, a transition between these two limiting values occurs. The functional form of the transition is determined by the nature of the distribution function. The results for the three different relaxation rate distributions are clearly distinguishable.

In Fig. 2(c), we re-plot Fig. 2(b) using a $1/T_W$ scale. On this scale, the derivatives of the linewidths with respect to $\ln T_W$ closely resemble the corresponding relaxation rate distributions. If the relaxation rate distribution falls off relatively slowly, as in curves 2 and 3, the data is essentially the relaxation rate distribution. Only curve 1, resulting from the step function distribution, shows appreciable modification of the underlying relaxation rate distribution function.

It should be noted that the fluctuations can originate from many different types of structural motions. Thus there could be some fine features on the flat relaxation rate distribution predicted by the simple TLS model. This has been observed recently in waiting time-dependent linewidth measurements in a chromophore–glass system.[30]

VI.2. Spin Flip Fluctuations in a Complex Crystal

In crystals with paramagnetic optical centers, optical dephasing can be induced by the fluctuations of electronic or nuclear spins

of the host lattice (or of the dopant, if the concentration is sufficiently high).[18,31] For a spin 1/2 system, the fluctuations (spin flips) correspond to transitions between two levels. Therefore, they are well described by the sudden jump model.

When the coupling between the optical center and the surrounding spins is weak, the flip rate is a constant, i.e., the relaxation rate distribution is a δ-function for a single type of spin. When the coupling between the optical center and the host spins is strong, the dynamics of the spins are affected by the existence of the optical center.[18] The strong coupling of nearby spins to the optical center detunes these spins from resonance with the bulk spins, and hence slows down their flip rates. The greater the coupling strength, the slower the flip rate. Since the coupling strength is dependent on the distance between the spin and the optical center, the flip rates are distributed over a broad range. In this case, the relaxation rate distribution is in the form of many peaks, because of the discrete nature of the lattice. As in glasses, two pulse echo and hole burning dephasing measurements have been observed to differ significantly in such complex crystals.[18]

In this subsection, we consider a set of elegant low temperature ($T \sim 2$ K) optical dephasing measurements performed on Pr^{3+}:CaF_2 crystals by Shelby and MacFarlane.[18] The perturbers of the optical center, Pr^{3+}, are spin 1/2 F^- nuclear spins, and the fluctuations involve spin flips. Since data are available and spin dynamics are relatively well understood, this example provides a concrete demonstration of the theory.

The experiment was performed on the $^1D_2$–$^3H_4$ (594.1 nm) optical transition of the Pr^{3+} ions. It was found that two pulse photon echo experiments measure a dephasing rate that corresponds to a homogeneous width of 370 kHz. Persistent hole burning, however, measures a hole width of 9 MHz.[18] Shelby and MacFarlane pointed out that the difference is caused by spectral diffusion induced by the relatively slow (compared to the optical dephasing time) spin flips of F^- nuclei. To support this explanation, they performed a transient spectral hole burning experiment using the technique of delayed optical free induction decay (FID). It is found that the dephasing rate of the delayed FID signal, which is related to the width of the hole, increases with the delay time, T_W, from 1 MHz at $T_W = 1$ μs, to 6 MHz at $T_W = 5$ ms.

Using the theory described in Section V, we were able to analyze the data quantitatively.[5] In this system, the Pr^{3+} has a strong ground state magnetic moment that detunes the nearby F^- spins from the bulk resonance and slows down their flip rates. Thus there is a broad distribution of flip rates, from the fastest bulk rate to the slowest rate that belong to the nearest spins.

To make the calculation manageable, we divide the F^- spins into three groups, and assume that the flip rates of the spins within each group can be approximated by a single rate. (1) The interstitial and the nearest neighbor F^- spins' flip rates are taken to be zero, because the maximum waiting time in the experiment, 5 ms, is several orders of magnitude shorter than the inverse of these flip rates ($\sim[\text{sec}]^{-1}$). (2) The F^- spins far away from the Pr^{3+} ion flip rates are taken to be the same as the free bulk rate R_0 ($\sim[\text{ms}]^{-1}$). (3) The F^- spins at intermediate distances flip rates are slower than R_0 but still significant on the experimental time scale. Because of the limited amount of data and for simplicity, we assume that the flip rates of this group can be replaced by a single rate R_1. We set the inner boundary of this last group of spins to be second nearest neighbors. The outer boundary is found in the fitting process to be somewhere between fourth and sixth nearest neighbors.

In effect, this assumes that the relaxation rate distribution can be approximated by three δ-functions. The flip rate of one of the δ-functions is set equal to zero. The flip rates of the other two δ-functions are free parameters to be determined in the fitting process.

Both the experimental data and the theoretical fit are plotted in Fig. 3. Note that there is a "dip" at about $T_W = 0.5$ ms. This is caused by the fact that the spectral diffusion is faster when a Pr^{3+} ion is in the excited state than when it is in the ground state. In the experiments, the dephasing rate is measured by FID. Both the ground state "hole" and the excited state population contribute to the FID signal. When the excited states relax to the ground state, the faster dephasing rate that they contribute to the signal vanishes. For times longer than the excited state lifetime, increased dephasing occurs only from the slower ground state spectral diffusion. Thus the hole width should first increase rapidly, drop, and then increase again more slowly. The fluorescence lifetime of this system is 509 μs, which is consistent with the observations.

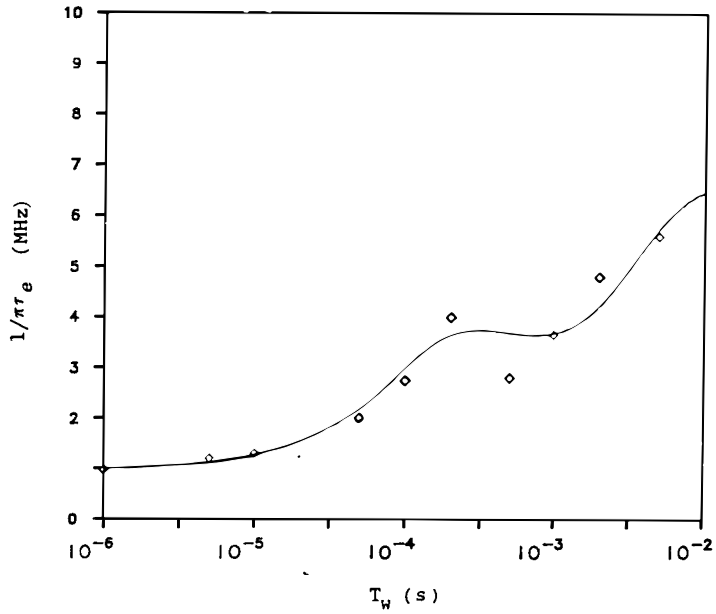

FIGURE 3 Fit of the delayed FID experimental data (Ref. 18) from Pr^{3+}:CaF_2 crystals. The vertical axis is $1/\pi\tau_e$, where τ_e is the $1/e$ point of the FID signal. The relaxation rate distributions are modeled as two δ-functions (see text), and the relaxation rates are varied to fit the data. Fitting parameters for the solid curve: $R_0 = 5.0\ [\text{ms}]^{-1}$, $R_1 = 0.35\ [\text{ms}]^{-1}$, and the boundary between spins with the two flip rates is the sixth nearest neighbor of the Pr^{3+}. All other parameters used in the calculation are experimentally measured values. The fit provides the relaxation rates, R_0 and R_1.

Except for the three free parameters, R_0, R_1, and the location of the boundary between the spins at intermediate distance and the "distant" spins, experimentally measured values[32] are used for all other parameters in the theoretical fit. The bulk F^- spin flip rate and the flip rate of the spins at intermediate distance are found to be $R_0 = 5\ [\text{ms}]^{-1}$ and $R_1 = 0.35\ [\text{ms}]^{-1}$, respectively. Considering the simplifications used to describe the relaxation rate distribution, the agreement between the data and the calculation is quite good. The calculation shows the flip rates of the F^- spins that contribute to the optical dephasing of Pr^{3+} ions fall predominantly in the range $0.35\ \text{ms}^{-1}$ to $5\ \text{ms}^{-1}$. The fundamental physics of the system is that spins close to the optical center are decoupled

from the bulk fluctuations by the hyperfine interaction with the Pr^{3+}. The real relaxation rate distribution is in the form of many δ-functions. There is a distinct relaxation rate for each lattice translation from the optical center until the distance is so large that the hyperfine interaction becomes negligible, and the rate becomes the bulk rate. By dividing the F^- spins into more spatial groups, i.e., by modeling the relaxation rate distribution with more δ-functions, we were able to fit the data essentially perfectly. However, given the limited amount of data, this procedure involves an unreasonable number of free parameters which obscure the basic physics of both the system and the experimental method. The simplifed rate distribution which was used gives the bulk flip rate, the distance over which the hyperfine interaction is important in modifying the flip rate, and an effective value for the flip rate of the perturbed spins.

VII. CONCLUSIONS

Optical dephasing or line narrowing measurements can reveal important information about dynamics in complex systems. However, the dynamics are not related to an optical lineshape in a manner described by conventional lineshape theory. The lineshape actually evolves over time. As a result, lineshapes can vary significantly when measured by different line narrowing techniques. We demonstrated that information about dynamics in complex systems can be extracted through the waiting-time-dependent measurement of the lineshape. In fact, it is the derivative of the linewidth with respect to the waiting time, T_W, which is directly related to the distribution of dynamical rates in a complex system. This conclusion applies to all systems where dynamics occur over broad temporal ranges. While optical line narrowing experiments have been discussed here, the same formalism applies to magnetic resonance experiments as well.

Acknowledgments

We would like to thank Dr. Robert Shelby for providing the details of the experiments on the Pr^{3+}:CaF_2 crystals and for his stimulating discussions with us about

the mechanism of optical dephasing in this system. This work was supported by the National Science Foundation Division of Material Research (DMR 87-18959), by the Office of Naval Research, Physics Division (N00014-85-K-0409), and by the Office of Naval Research (N00014-86-K-0825).

Y. S. BAI and M. D. FAYER
Chemistry Department,
Stanford University,
Stanford, California 94305

References

1. R. O. Pohl, in *Amorphous Solids: Low-Temperature Properties*, ed. W. A. Phillips (Springer, New York, 1981).
2. P. W. Anderson, B. I. Halperin and C. M. Varma, Phil. Mag. **25**, 1 (1972).
3. W. A. Phillips, J. Low Temp. Phys. **7**, 351 (1972).
4. M. J. Weber (Ed.), *Optical Linewidths in Glasses*, J. Lumin. **36**, 179 (1987).
5. Y. S. Bai and M. D. Fayer, Phys. Rev. B (to be published).
6. R. Kubo, in *Fluctuation, Relaxation and Resonance in Magnetic Systems*, ed. D. ter Haar (Oliver and Boyd, Edinburgh, 1962).
7. N. A. Kurnit, I. D. Abella and S. R. Hartmann, Phys. Rev. Lett. **13**, 567 (1964); J. Hegarty, M. M. Broer, B. Golding, J. R. Simpson and J. B. MacChesney, Phys. Rev. Lett. **51**, 2033 (1983).
8. E. L. Hahn, Phys. Rev. **80**, 580 (1950); T. W. Mossberg, R. Kachru, S. R. Hartmann and A. M. Flusberg, Phys. Rev. A **20**, 1976 (1979).
9. W. H. Hesselink and D. A. Wiersma, Phys. Rev. Lett. **43**, 1991 (1979); J. Chem. Phys. **75**, 4192 (1981).
10. Shuji Asaka, Hiroki Nakatsuka, Masahiro Fujiwara and Masahiro Matsoka, Phys. Rev. A. **29**, 2286 (1984); Norio Morita and Tatsuo Yajima, Phys. Rev. A **30**, 2525 (1984); R. Beach and S. R. Hartmann, Phys. Rev. Lett. **53**, 663 (1984).
11. M. J. Weber, in *Laser Spectroscopy of Solids*, ed. W. M. Yen and P. M. Selzer (Springer-Verlag, New York, 1981).
12. See, for example, M. D. Levenson, *Introduction to Nonlinear Laser Spectroscopy* (Academic Press, New York, 1982).
13. A. Szabo, Phys. Rev. Lett. **25**, 924 (1970).
14. See, for example, A. Abragam, *The Theory of Nuclear Magnetism* (Oxford University Press, New York, 1970).
15. D. E. McCumber and M. D. Sturge, J. Appl. Phys. **34**, 1682 (1963); J. L. Skinner and D. Hsu, Adv. Chem. Phys. **65**, 1 (1986).
16. C. A. Walsh, M. Berg, L. R. Narasimhan and M. D. Fayer, J. Chem. Phys. **86**, 77 (1987).
17. M. Berg, C. A. Walsh, L. R. Narasimhan, K. A. Littau and M. D. Fayer, J. Chem. Phys. **88**, 1564 (1988).
18. R. M. Macfarlane and R. M. Shelby, in *Laser Spectroscopy VI*, eds. H. P. Weber and W. Lüthy (Springer-Verlag, Berlin, 1983), p. 113; R. M. Shelby and R. M. Macfarlane, J. Lumin. **31 & 32**, 839 (1984).
19. S. Mukamel and R. F. Loring, J. Opt. Soc. Am. B **3**, 595 (1986); S. Mukamel, Phys. Rev. A **28**, 3480 (1983).
20. J. R. Klauder and P. W. Anderson, Phys. Rev. **125**, 912 (1962).
21. Y. S. Bai and M. D. Fayer, Chem. Phys. **128**, 135 (1988).

22. P. Hu and S. R. Hartmann, Phys. Rev. B **9**, 1 (1974); P. Hu and L. R. Walker, Phys. Rev. B **18**, 1300 (1978).
23. R. Maynard, R. Rammal and R. Suchail, J. Phys. Lett. **41**, L-291 (1980). Note that there is a numerical integral error in this reference. The value reported as 2.64 should be 3.6.
24. J. L. Black and B. I. Halperin, Phys. Rev. B **16**, 2879 (1977).
25. J. Hegarty, M. M. Broer, B. Golding, J. R. Simpson and J. B. MacChesney, Phys. Rev. Lett. **51**, 2033 (1983).
26. D. L. Huber, M. M. Broer and B. Golding, Phys. Rev. Lett. **52**, 2281 (1984); S. Hunklinger and M. Schmidt, Z. Phys. B **54**, 93 (1984).
27. See, for example, M. B. Weissman, Rev. Mod. Phys. **60**, 537 (1988).
28. T. Muramota, S. Nakanishi and T. Hashi, Opt. Comm. **24**, 316 (1978); K. K. Rebane and A. A. Gorokhovskii, J. Lumin. **36**, 237 (1987).
29. W. B. Mims, Phys. Rev. **168**, 378 (1968).
30. K. A. Littau, Y. S. Bai and M. D. Fayer, J. Chem. Phys., to be published (1989).
31. R. G. Devoe, A. Wokaun, S. C. Raud and R. G. Brewer, Phys. Rev. B **23**, 3125 (1981).
32. D. P. Burum, R. M. Shelby and R. M. Macfarlane, Phys. Rev. B **25**, 3009 (1982).